Genomics 95 (2010) 84–92

Contents lists available at ScienceDirect

Genomics

journal homepage: www.elsevier.com/locate/ygeno

Transition from compensated hypertrophy to systolic heart failure in the spontaneously hypertensive rat: Structure, function, and transcript analysis

Wesley W. Brooks [a,b,*], Steven S. Shen [c], Chester H. Conrad [a,b], Ronald H. Goldstein [a,b], Oscar H.L. Bing [a,b]

[a] From the VA Boston Healthcare System, 150 South Huntington Avenue, Boston, MA 02130, USA
[b] Department of Medicine, Boston University School of Medicine, Boston, MA 02118, USA
[c] Clinical and Translational Science Institute, Boston University School of Medicine, Boston, MA 02118, USA

ARTICLE INFO

Article history:
Received 20 August 2009
Accepted 5 December 2009
Available online 16 December 2009

Keywords:
Heart failure
Hypertension
Cardiac hypertrophy
Gene expression microarray

ABSTRACT

Gene expression, determined by micro-array analysis, and left ventricular (LV) remodeling associated with the transition to systolic heart failure (HF) were examined in the spontaneously hypertensive rat (SHR). By combining transcript and gene set enrichment analysis (GSEA) of the LV with assessment of function and structure in age-matched SHR with and without HF, we aimed to better understand the molecular events underlying the onset of hypertensive HF. Failing hearts demonstrated depressed LV ejection fraction, systolic blood pressure, and LV papillary muscle force while LV end-diastolic and systolic volume and ventricular mass increased. 1431 transcripts were differentially expressed between failing and non-failing animals. GSEA identified multiple enriched gene sets, including those involving inflammation, oxidative stress, cell degradation and cell death, as well as TGF-β and insulin signaling pathways. Our findings support the concept that these pathways and mechanisms may contribute to deterioration of cardiac function and remodeling associated with hypertensive HF.

Published by Elsevier Inc.

Background

The spontaneously hypertensive rat (SHR) is a useful laboratory model of genetic hypertension and naturally evolving hypertensive heart disease [1] that has enabled investigators to study changes in structure and function during the transition to heart failure (HF) [2-4].

More recent studies have shown alterations in cardiac gene expression in association with phenotypic changes related to ventricular remodeling associated with HF. Clinical studies of gene expression have been carried out in failing human hearts with coronary artery disease [5] and dilated cardiomyopathy [6]. Experimental studies have examined a number of models of HF , including transgenic rats with overexpression of the human renin (Ren) and angiotensinogen (Agt) genes [7], Dahl salt-sensitive rats [8,9], TNFα (Tnf) overexpressing mice [10], transgenic mice with compensated hypertrophy and HF [11], and dogs with chronic rapid ventricular pacing [12,13]. Differences with respect to identified transcripts have been described in different models of HF. When all transcript analysis of HF are taken together, however, a common HF profile emerges that appears to indicate that genes encoding transcription factors, remodeling/repair, the immune system, cell communication and cell death, including apoptosis, and stress response genes, were up-regulated [6–13] whereas potassium current transcripts [14,15], mitochondrial transcription factors, lipid and glucose metabolism transcripts [7,12,16–19] were down-regulated in failing compared to non-failing controls. Despite the many transcript changes found, the mechanism(s) underlying transition from adaptive cardiac hypertrophy to HF remains poorly understood.

Despite the importance of the SHR model, to our knowledge, only one study has been carried out using microarray gene chip analysis of the aging SHR to study HF [20]. This study compared differences between 12- and 16-month-old SHR with compensated LV hypertrophy and 20-month-old animals with diastolic dysfunction and HF; these SHR exhibited changes in diastolic properties of the heart, while systolic function was unimpaired. Changes were attributed to upregulation of the extracellular matrix (ECM) while the broad array of transcript changes found in other studies of HF [6–13,18,19] were not found. The apparent divergence between these findings and those in other models of HF may be related to differences between diastolic and systolic HF, species differences, or possibly differences in statistical analysis.

In an effort to improve the discovery of differentially expressed transcripts in the SHR with systolic HF, as demonstrated by LV and isolated papillary studies, individual LV samples from six SHR and six age-matched SHR with compensated hypertrophy were studied by micro-array gene expression analysis. In addition, Gene Set Enrichment Analysis (GSEA) was carried out in order to elucidate pathways involved [21].

* Corresponding author. VA Boston Health Care System (151), Research Building (R-127), 150 South Huntington, Avenue, Boston, MA 02130, USA.
E-mail addresses: wesley.brooks@va.gov, brooksww@bu.edu (W.W. Brooks).

0888-7543/$ – see front matter. Published by Elsevier Inc.
doi:10.1016/j.ygeno.2009.12.002

Results

Development of HF

Sixteen 12-month-old SHR were initially entered into the study; four died prior to study. Of the surviving twelve SHR, six developed evidence of HF (SHR-F), and were compared to six additional SHR without HF (SHR-NF). Animals were considered to have HF when based on documentation of left ventricular dysfunction echocardiography findings, specifically LV enlargement with LV ejection fraction <55% (normal >80%). Pathological findings associated with heart failure included pleural and/or pericardial effusions, left atrial or LV thrombi, and right ventricular hypertrophy, as described previously [3,4,22–24]. Peak systolic blood pressure was 145 ± 8 mm Hg in SHR-F, as compared to 185 ± 5 mm Hg in SHR-NF. The mean age at the time of study (19 ± 1 months) was not significantly different between groups.

Echocardiography

Serial echocardiographic measurements of LV ejection fraction (LVEF) and LV volumes were carried out beginning at 12 months of age and approximately every 8 weeks thereafter until the development of HF. LVEF in 12-month-old animals (without HF) is approximately 90%, gradually declined with age to approximately 83 to 84% in non-failing SHR at 17 months of age, and to 54.2 ± 4% with HF. Echocardiographic findings of SHR hearts without HF (SHR-NF) and SHR at the time of HF (SHR-F) are presented in Table 1. LV ejection fraction and fractional shortening, used as measures of systolic function, decreased significantly, while LV end-diastolic and end-systolic chamber dimensions increased with HF (Fig. 1).

Pathological parameters

Body weight, cardiac chamber weights, and chamber weights normalized for body weight are presented in Table 2. Body weight decreased, and the LV and, to a greater extent, RV weight increased in SHR with HF relative to non-failing SHR ($p<0.01$). Body weight was significantly reduced ($p<0.05$), and LV/BW and RV/BW ratio significantly increased, in SHR-F relative to SHR-NF. Myocardial and liver water content data is also presented in Table 2. Left ventricular and liver water content (expressed as g water/g dry wt) was increased in SHR with HF compared to SHR with compensated hypertrophy ($p<0.05$).

Isolated muscle data

Isometric papillary muscle data from SHR-NF and SHR-F are summarized in Table 3; peak active isometric stress and quick-release force–velocity relationships are presented in Fig. 2. Papillary muscle cross-sectional area was not significantly different between SHR groups. In SHR-F, active isometric stress (σ_{active}, active developed tension normalized for muscle cross-sectional area) and maximum rate of stress development ($+d\sigma/dt$) were depressed, and relaxation time significantly abbreviated, relative to SHR-NF. Myocardial stiffness was significantly increased in SHR-F compared to SHR-NF (Table 3). Velocity of shortening was less at all loads examined in papillary muscles from SHR-F than SHR-NF ($p<0.01$).

Table 1
Echocardiographic measurements.

	SHR-NF		SHR-F	
	Initial	Time of study	Initial	Time of study
LVEF%	89.2 ± 6.0	83.7 ± 5.2	90.9 ± 4.4	54.2 ± 4.5*
LVFS%	55.5 ± 5.5	46.8 ± 7.8	56.7 ± 5.3	23.1 ± 2.6*
$LVEDD_{mm}$	7.32 ± 0.66	7.54 ± 0.78	7.23 ± 0.89	9.75 ± 0.72*
$LVESD_{mm}$	3.40 ± 0.39	4.00 ± 0.66	3.25 ± 0.41	7.45 ± 0.69*
$EDVtz_{ml}$	0.89 ± 0.22	0.98 ± 0.27	0.88 ± 0.32	1.93 ± 0.40*
$ESVtz_{ml}$	0.14 ± 0.06	0.17 ± 0.07	0.10 ± 0.05	0.93 ± 0.24*

SHR-NF indicates spontaneously hypertensive rats without HF, initial echocardiographic data obtained at 12 months of age, and at time of study; SHR-F, spontaneously hypertensive rats with HF, initial echocardiographic data obtained at 12 months of age, and at time of study. LVEF, left ventricular ejection fraction; LVFS, left ventricular fractional shortening; LVEDD, left ventricular end-diastolic diameter; LVESD, left ventricular end-systolic diameter; EDVtz, end-diastolic volume (Teichholz); ESVtz, end-systolic volume (Teichholz).
Values are mean of six rats per group ± SD. *$p<0.05$ SHR-F vs. SHR-NF at the time of study.

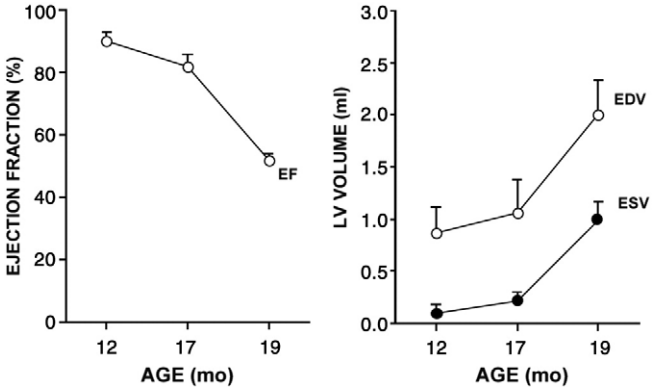

Fig. 1. Serial echocardiographic measurements in SHR. LV ejection fraction (left panel) and end-systolic and end-diastolic LV volume (right panel) of male SHR during the transition to heart failure (12, 17, and 19 months of age). EF, indicates LV ejection fraction (%); ESV, end-systolic volume (ml; black circle); EDV, end-diastolic volume (ml; open circle). LV function remains compensated until approximately 17 months, and then rapidly declines; mean age at onset of HF 19 ± 1 months.

Response to β-adrenergic stimulation

Peak σ, $+d\sigma/dt$, and time to peak σ were determined at muscle bath isoproterenol (ISO) concentrations of 10^{-8} and 10^{-7} mmol/l. In SHR-F, 10^{-7} ISO decreased peak σ by 16 ± 2% of pre-ISO control, and $+d\sigma/dt$ was unchanged. In SHR-NF, peak σ was unchanged and $+d\sigma/dt$ increased by 14 ± 4% at 10^{-7} ISO. Time to peak σ and relaxation time index decreased by approximately 15% and 25%, respectively, with ISO in both groups (NS).

Histology

Fig. 3 is a cross-section of the LV from SHR-NF and SHR-F stained with Masson's trichrome. Representative sections of LV-free wall and LV papillary muscles from SHR-NF and SHR-F were assessed by quantitative histological analysis. Table 4 presents quantitative connective tissue and myocyte area data. Myocardial fibrosis was increased in LV and papillary muscle samples from SHR-F relative to SHR-NF ($p<0.05$) and to a greater extent relative to age-matched normotensive WKY (LV average 8.3 ± 4.0%; WKY data not shown).

Differentially expressed LV transcripts between SHR-F and SHR-NF

A total of 1,431 transcripts were found to be differentially expressed in LV samples from SHR-F relative to SHR-NF ($p<0.05$) by microarray analysis. Of these, 484 transcripts (294 upregulated and 190 downregulated) were positively identified with known biological function. Fig. 4 is an example of four highly expressed transcripts that were down- and five up-regulated with HF, obtained from six individual LV samples from SHR-F (left panel) and SHR-NF (right panel). In general, the extent of expression changes appeared to be related to the extent of myocardial impairment. The top 25 identified transcripts that were most substantially up- and down-regulated are presented in Tables 5 and 6, respectively. (See supplemental tables for a complete list of all identified transcripts differentially expressed with HF).

Table 2
Cardiac chamber weight, body weight, ratios and tissue water content.

	LV (g)	RV (g)	BW (g)	LV/BW (mg/g)	RV/BW (mg/g)	LV/TL (mg/cm)	LV (wet/dry)	Liver (wet/dry)
SHR-NF	1.36 ± 0.12	0.24 ± 0.03	404 ± 27	3.36 ± 0.34	0.59 ± 0.09	0.32 ± 0.02	3.68 ± 0.09	2.22 ± 0.27
SHR-F	1.43 ± 0.14	0.40 ± 0.06^{+}	366 ± 24^{+}	3.90 ± 0.33*	1.11 ± 0.17^{+}	0.36 ± 0.03	3.85 ± 0.14*	2.58 ± 0.15*

LV, left ventricular weight; RV, right ventricular weight; BW, body weight; LV/BW, left ventricular weight to body weight ratio; RV/BW, right ventricular weight to body weight ratio; LV/TL, left ventricular weight to tibia length ratio; LV, left ventricular water content expressed as g water/g dry tissue wt; Liver, water content expressed as g water/g dry tissue wt.
Data are mean of 6 rats per group ± SD. *p<0.05 SHR-F vs. SHR-NF; +p<0.01 SHR-F vs. SHR-NF.

Findings of individual transcripts indicate decreases in metabolic regulatory enzymes (e.g. pyruvate dehydrogenase kinase (Pdk2), glycerol-3-phosphate dehydrogenase 2 (Gpd2), phosphofructokinase (Pfkm) and phosphoglycerate mutase 2 (Pgam2)). Several transcripts involved in fatty acid oxidation were decreased with HF (e.g. enolyl-coenzyme A, hydratase/3-hydroxyacyl coenzyme A dehydrogenase (Ehhadh), acyl-coenzyme A dehydrogenase; and, solute carrier family 25, carnitine acetytransferase (S1c25a20) and carnitine palmitoyl-transferase 2 (Cpt2), and L-3-hydroxyacyl-Coenzyme A dehydrogenase, short chain (Hadh)). In addition, cardiac and mitochondrial specific 3-hydroxybutyrate dehydrogenase (Bdh1) and adenosine triphosphate cassette transporter were significantly downregulated in the SHR-F group. The signal transduction gene RASD member 2 (Rasd2) was also markedly downregulated in the LV from SHR-F relative to compensated SHR.

The most highly down-regulated transcripts found in the SHR-F vs. SHR-NF were related to cardiac contractile apparatus and included myosin, heavy polypeptide 7 (Myh7), cardiac muscle, beta and myosin heavy chain, polypeptide 6. On the other hand, the most highly expressed transcript of the LV from the SHR-F group was the immunomodulatory gene lipopolysaccharide binding protein (Lbp). Nuclear protein 1 (Nupr1), a transcription factor associated with the induction of apoptosis, was also highly expressed in the SHR-F group.

Expression of the extracellular matrix (ECM) related transcripts fibronectin (Fn1), lysyl oxidase (Lox), and cathepsin S (Ctss) was significantly elevated in the SHR-F vs. SHR-NF. Several transcripts often associated with human HF (e.g. arginine-vasopressin (Avp), dopamine hydroxylase (Dbh), and transcripts involved in tumor necrosis factor-α (Tnf) and transforming growth factor beta-1 (Tgfb1) signaling pathways) were also found to be up-regulated in the SHR-F group.

Gene function and pathway enrichment with systolic HF

The functional outcomes of the GSEA and GO-based analysis are summarized in Table 7. In gene sets C2 collection (SHR with HF vs. age-matched, SHR without HF), a total of 1,340 gene sets were tested. In this analysis, 993 gene sets were upregulated and 347 genes sets were downregulated with systolic HF. A total of 83 pathways and curated signature related gene sets were significantly enriched in terms of nominal p-value less than 0.01 (See supplemental tables for pathway details). Pathways involving TGF-β and insulin signaling were highly enriched. Additional gene sets that were altered with HF include oxidative stress, complement and coagulation pathways, cell and structure degradation, apoptosis, metabolism, cell adhesion, and inflammation.

Table 3
Isolated papillary muscle parameters.

	CSA (mm^2)	$+d\sigma/dt$ ($g/mm^2/s$)	TPS (ms)	$RT_{1/2}$ (ms)	Kcs (stiffness)
SHR-NF	1.4 ± 0.37	43.1 ± 8.6	176 ± 20	188 ± 14	53 ± 4
SHR-F	1.42 ± 0.39	22.2 ± 6.8*	184 ± 13	144 ± 14*	74 ± 15*

CSA, indicates cross-sectional area of LV papillary muscle; $+d\sigma/dt$, rate of stress development; TPS, time to peak stress; $RT_{1/2}$, relaxation time index; Kcs, myocardial stiffness constant. Data are mean of six papillary muscles per group ± SD. *p<0.05 SHR-F vs. SHR-NF.

Gene sets C5 collection, a total 926 gene sets were tested (564 gene sets upregulated and 362 gene sets downregulated with HF). A total of 34 GO term function related gene sets were significantly enriched at the level of nominal p-value less than 0.01 (Table 8). Overexpressed GO classes of the LV from failing SHR most prominent of which were biological processes involved in cell signaling pathways, binding of cellular constituents and cell death. The enriched gene sets which meet criteria of nominal p-value less than 0.05 are provided as supplements.

Confirmation of expression changes

To validate changes in transcripts from microarray data, quantitative PCR was performed on a subset of transcripts from SHR-NF and SHR-F (Table 9). Ten transcripts were selected for quantitative analysis; seven were up-regulated with HF by gene chip analysis (i.e. lipopolysaccharide binding protein (Lbp), cathepsin S (Ctss), lysyl oxidase (Lox), dopamine beta-hydroxylase (Dbh), arginine vasopressin (Avp), cAMP response element modulator (Crem), and programmed cell death 4 (Pdcd4)), and three genes were down-regulated (i.e. RASD family member 2 (Rasd2); L-3-hydroxyacyl-Coenzyme A dehydrogenase, short chain (Hadh); and acyl-Coenzyme

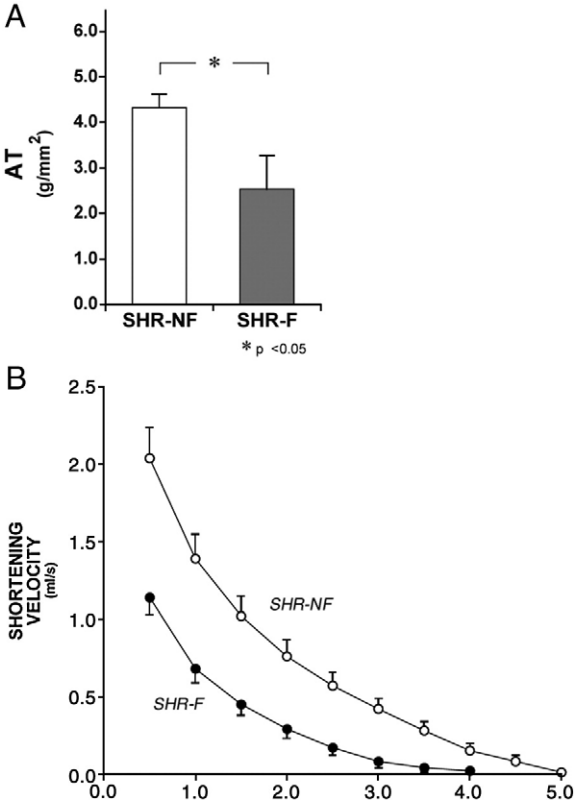

Fig. 2. (A) Active tension (AT) of LV papillary muscles. AT was significantly depressed (p<0.01) in SHR-F in comparison to SHR-NF. (B) Quick release force–velocity (F–V) relationships from LV papillary muscles. F-V relationships were significantly depressed (p<0.01) in SHR-F in comparison to SHR-NF. Data are mean ± SD (n = 6 per group).

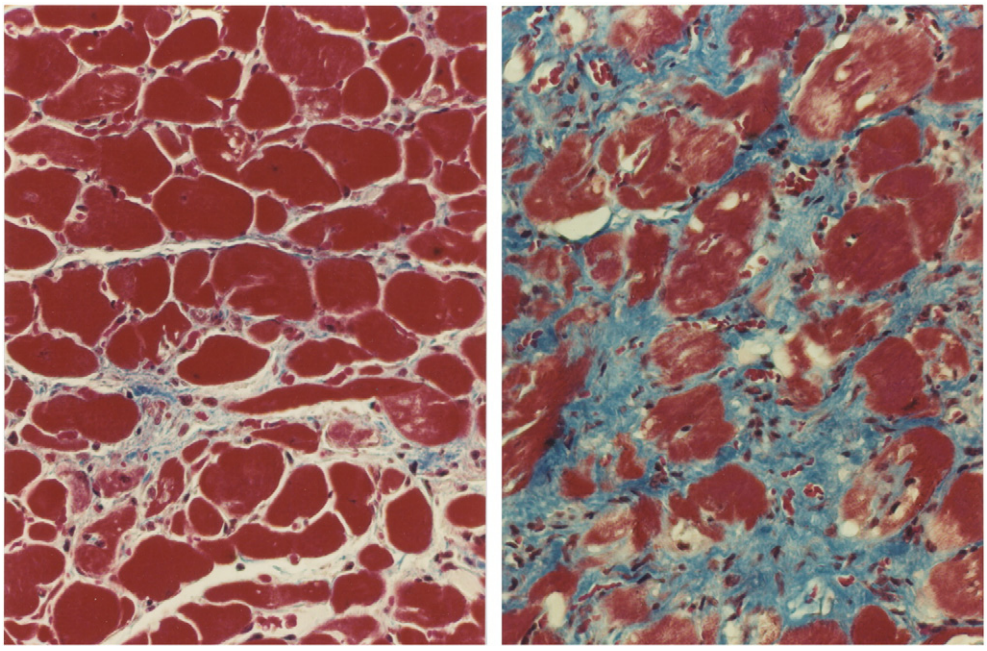

Fig. 3. High power (25×) cross-section stained with Masson's trichrome from non-failing SHR (left panel) and SHR with HF (right panel). The sections were obtained half way between LV apex and base. There is marked fibrosis of the LV from SHR-F.

A oxidase 2, branched chain (Acox2)). Overall, transcript changes with HF, as determined by microarray analysis, were qualitatively consistent with the results obtained by real-time PCR, and corroborate our microarray findings. The immunomodulatory transcript Lbp was the most highly correlated transcript determined by RT-PCR and microarray analysis ($r = 0.94$; $p < 0.0001$).

Functional correlates

The level of Lbp expression, which was markedly up-regulated in the LV by microarray and RT-PCR with HF, was negatively correlated ($r = -0.76$; $p = 0.004$) to maximum active tension developed by LV papillary muscles from the same heart (Fig. 5A. Increased myocardial stiffness associated with HF was directly correlated ($r = 0.70$; $p = 0.0169$; Fig. 5B) to the expression level of lysyl oxidase (Lox) from individual papillary muscles determined by microarray and RT-PCR. Thus, the extent of myocardial dysfunction of LV papillary muscles correlated with LV expression of the immunomodulatory transcript Lbp and the collagen-cross linking enzyme lysyl oxidase (Lox).

Discussion

Cardiac phenotype

This study defines changes in the SHR heart during the transition to systolic HF. Pathologic assessment of the heart reveals LV and RV hypertrophy, fibrosis and increased LV water content in the SHR-F compared with age-matched SHR-NF, consistent with prior studies [3,4,22–24]. Echocardiographic data demonstrate a reduction in LV ejection fraction and an increase in LV diastolic and systolic dimensions in the SHR-F (see Table 1). An analysis of isolated LV

Table 4
Histological analysis.

	n	LV papillary muscles		LV free wall
		Myocyte (fractional area,%)	Connective tissue (fractional area,%)	Connective tissue (fractional area,%)
SHR-NF	6	69.8 ± 6.8	16.2 ± 2.0	12.1 ± 1.6
SHR-F	6	64.9 ± 3.7	21.9 ± 2.8*	19.1 ± 1.6*

Histological findings (myocytes, connective tissue) expressed as a % of total area from analysis of cross-sections of LV papillary muscles and LV free wall samples. These data are from SHR in which physiological and gene expression studies were carried out. Values are mean ± SD.
* $p < 0.05$ SHR-F vs. SHR-NF.

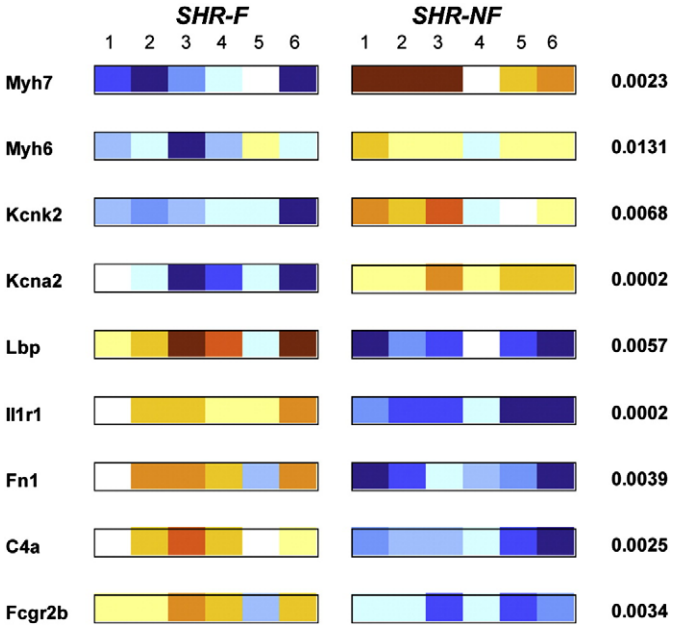

Fig. 4. Individual expression levels of transcripts from the LV of SHR with and without HF. Examples of several structural and functional transcripts that were significantly down-regulated with HF (top four) and cell defense (i.e. immune and inflammatory transcripts) that were up-regulated with HF (bottom five). Myh7, indicates myosin, heavy polypeptide 7, cardiac muscle, beta; Myh6, myosin heavy chain, polypeptide 6; Kcnk2, potassium channel, subfamily K, member 2; Kcna2, potassium voltage-gated channel, shaker-related subfamily, member 2; Lbp, lipopolysaccharide binding protein; Il1r1, interleukin 1 receptor, type I; Fn1, fibronectin 1; C4a, complement component 4a; Fcgr2b, Fc receptor, IgG, low affinity IIb. The blue colored samples represent lower expression levels while red indicates higher expression. White indicates no changes in mRNA-expression occurred. Statistical significance comparing SHR-F to SHR-NF values is presented in the last column.

Table 5
Top 25 transcripts that were significantly up-regulated with HF ($p<0.05$). Up-regulated transcripts ranked by fold change.

Identifier	Gene title	p	Fold change			
			FDR	F/NF	Function	Chrom.
BF289368	Lipopolysaccharide binding protein	0.0057	0.0115	6.11	CD	2
AB001382	Secreted phosphoprotein 1	0.0139	0.0251	4.37	CS	5
NM_013123	Interleukin 1 receptor, type I	0.0002	0.0091	3.95	CD	1
BG380575	Neuronal pentraxin receptor	0.0001	0.0065	3.72	TT	15
AA893484	Fibronectin 1	0.0039	0.0135	3.65	S/CD	1
NM_031521	Neural cell adhesion molecule 1	0.0017	0.0122	3.58	CA/TT	9
BI285347	Complement component 4a	0.0025	0.0129	3.56	CD	17
AF187814	Camello-like 3	0.0005	0.0092	3.4	TT	6
U23438	Dual specificity phosphatase 4	0.0004	0.0092	3.37	CS	8
AI179988	Ectodermal-neural cortex 1	0.0077	0.0181	3.24	CA/PM	13
AA850692	Activin receptor interacting protein 1	0.0009	0.0114	3.24	CS	5
AI230669	Guanine nucleotide binding protein, beta 1	0.0335	0.0486	3.17	CS	4
NM_053433	Flavin containing monooxygenase 3	0.0083	0.0185	3.14	EM	1
NM_053611	Nuclear protein 1	0.0015	0.0116	3.11	TT	7
X89963	Thrombospondin 4	0.0014	0.0118	3.09	CA	13
NM_053326	Enigma homolog	0.0010	0.0113	2.96	CS	3
NM_031832	Lectin, galactose binding, soluble 3	0.0035	0.0136	2.9	CA/PM	14
AF202115	Ceruloplasmin	0.0118	0.0226	2.79	T	3
NM_012620	Serine (or cysteine) proteinase inhibitor, clade E, member 1	0.0181	0.0301	2.77	CS/TT	5
NM_012620	Serine (or cysteine) proteinase inhibitor, clade F, member 1	0.0062	0.0161	2.77	CS/TT	11
X73371	Fc receptor, IgG, low affinity IIb	0.0034	0.0135	2.75	CD	1
AA850991	Chondroitin sulfate proteoglycan 2	0.0008	0.0111	2.75	CA	13
AI407489	Solute carrier organic anion transporter family, member 2a1	0.0016	0.0121	2.75	T	9
BF419200	CCAAT/enhancer binding protein (C/EBP), delta	0.0005	0.0091	2.73	TT	16
NM_021586	Latent transforming growth factor beta binding protein 2	0.0082	0.0184	2.73	CS	12

B, Biosynthesis/general metabolism; CA, cell adhesion or binding activity; CD, cell defense (i.e. immunity/oxidative stress); CS, cell signaling/communication; D, death associated; G, cell growth/maintenance; EM, energy metabolism; PM, protein or structural modifier; S, cell structure (i.e. ECM) or function (i.e. contraction); T, transport; TT, transcription/translation regulatory activity; O, other unclassified function. Chrom indicates chromosome location. The same format applies for Tables 5 and 6.

papillary muscle function demonstrates depressed active tension and shortening velocity, and increased myocardial stiffness, in SHR-F compared with SHR-NF (Table 3). These findings support the concept that depressed cardiac function, demonstrated by echocardiography, is due to impaired intrinsic contractile properties of the myocardium.

Changes in LV gene expression

Previous transcriptomic studies of various HF models have noted differences in the number and profile of identified transcripts. For example, HF in the TNFα overexpressing mouse model is characterized by an increase in expression of inflammatory cytokines [10] Dahl salt-sensitive rats exhibit an increase in apoptosis transcripts [8,9]. Microarray gene expression profiles of HF due to dilated hypertrophic cardiomyopathy have been associated with down-regulation of SR/endoplasmic reticulum and Ca2+-ATPase transcripts, and the upregulation of ECM transcripts [5]. Studies of pacing induced HF found that energy and metabolism-related transcripts were down-regulated with HF [12], and oxidative stress transcripts were upregulated [13]. Taken together, however, studies in general indicate that genes encoding transcription factors, remodeling/repair, the immune system, cell communication and cell death, including apoptosis, and stress response genes, were up-regulated [6–9,12,13] whereas potassium current transcripts [14,15], mitochondrial transcription factors, lipid and glucose metabolism transcripts [7,12,16–19] were down-regulated in failing compared to non-failing controls. (For a systemic review of large scale and heterogenous gene array data in HF see [25]).

A previous study employing DNA microarray analysis of the aging SHR found that relatively few transcripts were altered during the development of diastolic dysfunction [20]. In their study, differences between 12- and 16-month-old SHR with compensated LV hypertrophy were compared to 20-month-old animals with diastolic dysfunction; findings included increases in extracellular matrix (ECM) transcripts, while differences in calcium homeostasis, contractile, cytoskeletal, neurohumoral and energy transcripts were not found. These apparent divergence between these findings and those in other models of HF may be related to differences between diastolic and systolic HF, species differences, or possibly differences in statistical analysis, in that small sample sizes may limit sensitivity for identification of changes.

In the present study, initial microarray analysis indicated a total of 1,431 transcripts were differentially expressed with HF of which, 484 (294 up regulated and 190 down-regulated) transcripts were positively identified. The immunomodulatory gene lipopolysaccharide binding protein (Lbp) was the single most highly expressed transcript (i.e. greater than 6 fold increase) in failing relative to non-failing LV, and was negatively correlated to force generation when compared with papillary muscle function from the same LV (R −0.76; Fig. 5A). When compared to age-matched, normotensive WKY rats, Lbp expression in LV from the SHR-F group was more than 26-fold greater (unpublished observation). Lbp also has been found to be the most highly expressed transcript with systolic dysfunction induced by coronary artery occlusion [26]. Together, these findings suggest that up-regulation of expression of mediators of inflammation are a common features in these two models of systolic dysfunction, and that Lbp expression might potentially serve as a biomarker of myocardial dysfunction.

An upregulated immune and inflammatory response is well recognized to be a feature of the pathophysiology of chronic HF resulting from many causes [27]. Elevated expression of inflammatory cytokines TNF-α and TGF-β_1 have been demonstrated in patients with severe HF [27,28], and in the SHR [24,29,30]. Inflammation and the inflammatory cytokine TGF-β_1, in particular, has been shown to alter lipid metabolism and decrease fatty acid oxidation in the kidney [31] and heart [32] which may account, in part, for the downregulation of transcripts involved in energy metabolism and fatty acid oxidation found in the SHR with HF.

A 2.5-fold elevation of cathepsin S (Ctss) transcripts was found in the SHR-F group. Cathepsin S, a cysteine protease, plays a role in the degradation of peptide chains; in particular those associated with the immune response [33], and has been shown to participate in pathological remodeling of the LV associated with hypertension-induced HF in humans and rats [34]. Thus, cathepsin S may contribute to adverse LV remodeling found in the SHR-F.

The largest transcript decline was found in the cardiac muscle contractile protein myosin, heavy polypeptide 7. Increased beta-myosin heavy chain gene expression is associated with the development of cardiac hypertrophy and mutations in this gene have been

Table 6
Top 25 transcripts that were significantly down-regulated with HF ($p<0.05$). Down-regulated transcripts ranked by fold change.

Identifier	Gene title	p	Fold change			
			FDR	F/NF	Function	Chrom.
AI535411	Myosin, heavy polypeptide 7, cardiac muscle, beta	0.0023	0.0125	0.18	S	14
AI103845	UDP-N-acetyl-alpha-D-galactosamine: polypeptide N-acetylgalactosaminyltransferase 13	0.0035	0.0136	0.27	PM	2
AF385402	potassium channel, subfamily K, member 2	0.0068	0.0167	0.33	T	1
AA943734	mitochondrial protein, 18 kDa	0.0013	0.0117	0.34	S	11
M74449	potassium voltage-gated channel, shaker-related subfamily, member 2	0.0002	0.0092	0.34	T	
AF134409	RASD family, member 2	0.0017	0.0122	0.35	CS/TT	8
NM_031730	potassium voltage gated channel, Shal-related family, member 2	0.0038	0.0136	0.37	T	6
BE098261	solute carrier family 25 (mitochondrial oxodicarboxylate carrier), member 21	0.0013	0.0116	0.37	T	12
J02997	dipeptidylpeptidase 4	0.0002	0.0087	0.42	D	2
BG378827	putative chloride channel	0.0144	0.0256	0.43	T	7
BI295768	LRP16 protein	0.0110	0.0200	0.46	TT	19
NM_022604	endothelial cell-specific molecule 1	0.0005	0.0093	0.46	G	13
AW525609	inositol (myo)-1(or 4)-monophosphatase 2	0.0034	0.0135	0.47	O	18
NM_019174	carbonic anhydrase 4	0.0022	0.0124	0.47	B	11
AI170387	chemokine (C-X-C motif) ligand 9	0.0032	0.0133	0.48	CD	5
BF555973	triadin	0.0275	0.0415	0.49	S	10
BE098261	solute carrier family 25 (mitochondrial oxodicarboxylate carrier) member 11	0.0139	0.0251	0.50	T	11
NM_033352	ATP-binding cassette, sub-family D(ALD), member 2	0.0086	0.0186	0.51	T/EM	15
NM_017239	myosin heavy chain, polypeptide 6, cardiac muscle, alpha	0.0131	0.0243	0.52	S	14
AA799574	L-3-hydroxyacyl-Coenzyme A dehydrogenase, short chain	0.0061	0.0160	0.52	EM	3
X95189	acyl-Coenzyme A oxidase 2, branched chain	0.0048	0.0143	0.52	EM	14
BF420810	histidine rich calcium binding protein	0.0087	0.0189	0.52	CA	7
AI411446	pyruvate dehydrogenase phosphatase isoenzyme 2	0.0018	0.0122	0.53	EM	8
NM_012506	ATPase Na+/K+ transporting, alpha 3 polypeptide	0.0139	0.0251	0.53	T/EM	7
NM_080399	DNA-damage-inducible transcript 4	0.0218	0.0349	0.53	TT/D	10

found responsible for genetic dilated cardiomyopathy and HF in humans [35]. Down-regulation of myosin, heavy chain polypeptide genes has been noted in the LV from canine tachycardia-induced HF [12] and rats with HF following myocardial infarction [36]. The functional consequences of specific contractile protein changes in different models of HF, however, remains to be determined.

Studies have suggested that oxidative stress is enhanced in HF [37]. Free radical formation can affect transcripts regulating ion channels, Ca^{2+} homeostasis, mitochondrial function, transcription factors, DNA binding activity, growth, and apoptosis [38], and has been shown to induce myocyte hypertrophy, apoptosis, and interstitial fibrosis [37]. In the present study, oxidative stress genes were up-regulated while PPAR gamma (Pparg), a regulator of myocardial superoxide content and redox homeostasis [39], was downregulated. The expression level of aldehyde dehydrogenase, a source of cytosolic reactive oxygen species [40] from the LV, was negatively correlated with active force of individual papillary muscles from the same heart ($R=-08877$, $p<0.001$). Findings appear consistent with a role for oxidative stress in the failing SHR heart.

Our findings from gene set enrichment analyses provide additional insight into the expression profiles associated with systolic HF progression, such as the enrichment of gene sets involved in TGF-β and insulin signaling pathways. Upregulation of TGF-β signaling was identified by the outcome of GSEA pathway and GO-based analysis. Increased TGF-β_1 mRNA has been found in the LV from aging SHR during the transition to HF [24,29]. TGF-β and insulin-like growth factor transcripts have been reported to be upregulated in cardiac

Table 7
Curated summary of pathway changes with HF.

Gene set name	Size	ES	NES	NOM
UP with HF				
Insulin signaling	17	0.700	1.899	0.000
LVAD_heart failure	63	0.595	1.862	0.000
TGF-β signaling pathway	41	0.630	1.832	0.000
IFN beta signaling	38	0.462	1.843	0.000
Oxidation (Passerini)	17	0.629	1.785	0.000
Complement and coagulation cascades	59	0.589	1.850	0.002
HDAC inhibition	56	0.448	1.661	0.002
Wnt targets	19	0.675	1.843	0.002
Adhesion (Passerini)	36	0.619	1.665	0.002
INOS	72	0.424	1.850	0.004
Apoptosis (Passerini)	36	0.408	1.527	0.006
Inflammation (Passerini)	25	0.588	1.743	0.008
Down with HF				
Myc signaling (Coller)	15	0.700	1.810	0.000
Alanine and aspartate metabolism	20	0.520	1.550	0.002
Glycerophospholipid metabolism	53	0.350	1.440	0.006

GSEA on SHR with HF vs. SHR without HF gene sets, enriched known pathways and gene signatures in systolic HF (NOM p-value<1%). Size, size of gene set; ES, enrichment score; NES, normalized enrichment score; NOM p-value, nominal p-value. Analysis as previously described (Subramanian et al. [21]). Recently updated gene sets (MSigDB, version 2.5) were utilized for GSEA analysis. The array data from total six replicated samples in failure condition was computed against samples in control group based on GSEA algorithm.

Table 8
Curated summary of transcriptomic changes with HF.

Gene set name	Size	ES	NES	NOM
UP with HF				
Glycosaminoglycan binding	25	0.681	1.874	0.000
Carbohydrate binding	50	0.525	1.847	0.000
TGF-β signaling pathway	31	0.596	1.772	0.000
Nitrogen compound metabolic process	131	0.308	1.389	0.000
Endoplasmic reticulum	241	0.293	1.526	0.002
Proteolysis	154	0.361	1.663	0.006
Phagocytosis	15	0.641	1.654	0.006
Regulation of cell signaling	175	0.396	1.521	0.006
Cation binding	172	0.312	1.510	0.007
Down with HF				
Organellar ribosome	19	0.796	1.577	0.002
Mitochodrial ribosome	19	0.796	1.577	0.002
Cofactor biosynthetic process	19	0.667	1.635	0.004

GSEA on SHR with HF vs. SHR without HF gene sets overrepresented GO classes of biological processes in systolic HF (NOM p-value<1%). Size, size of gene set; ES, enrichment score; NES, normalized enrichment score; NOM p-value, nominal p-value. Analysis as previously described (Subramanian et al. [21]). Recently updated gene sets (MSigDB, version 2.5) were utilized for GSEA analysis. The array data from total six replicated samples in failure condition was computed against samples in control group based on GSEA algorithm.

Table 9
Real-time RT-PCR and differential expression results from microarray experiments.

Gene	RT-PCR		Microarray
	Fold change	*p* Value	Fold change
Up-regulated			
Lbp	4.85	NS	6.11
Ctss	2.65	NS	2.5
Lox	2.85	NS	2.41
Dbh	**10.18**	**>0.05**	**1.41**
Avpi1	1.73	NS	1.60
Crem	1.24	NS	1.49
Pdcd4	1.55	NS	1.49
Down-regulated			
Rasd2	0.46	NS	0.35
Hadhsc	0.71	NS	0.51
Acox2	0.49	NS	0.52

Confirmation of the microarray gene expression for ten randomly selected genes by RT-PCR. Ratio of expression for each gene in SHR-F group to age-matched SHR without HF. Fold, relative fold changes as assessed by real-time RT-PCR and microarray. Fold change above 1 denotes upregulated, and fold change below 1 denotes downregulated expression. p-value, indicates $p<0.05$ of RT-PCR relative to assessment by microarray. Bold letters highlights genes with result discrepancy between RT-PCR and microarray values. Lbp, indicates lipopolysaccharide binding protein; Ctss, cathepsin S; Lox, lysyl oxidase; Dbh, dopamine beta-hydroxylase; Avpi1, arginine vasopressin; Crem, cAMP response element modulator; Pdcd4, programmed cell death 4; Rasd2, RASD family member 2; Hadhcs, L-3-hydroxyacyl-Coenzyme A dehydrogenase, short chain; and Acox2, acyl-Coenzyme A oxidase 2, (branched chain).

tissue after acute myocardial infarction [26]. In addition, GSEA analysis identified enriched gene sets involving inflammation, oxidative stress and cell death (Tables 7 and 8, and supplemental tables). GSEA analysis also identified similarities to human HF prior to ventricular unloading with an LV assist device [41]. This finding is of interest considering the increasing recognition of the role of immune and inflammatory systems in the genesis of HF.

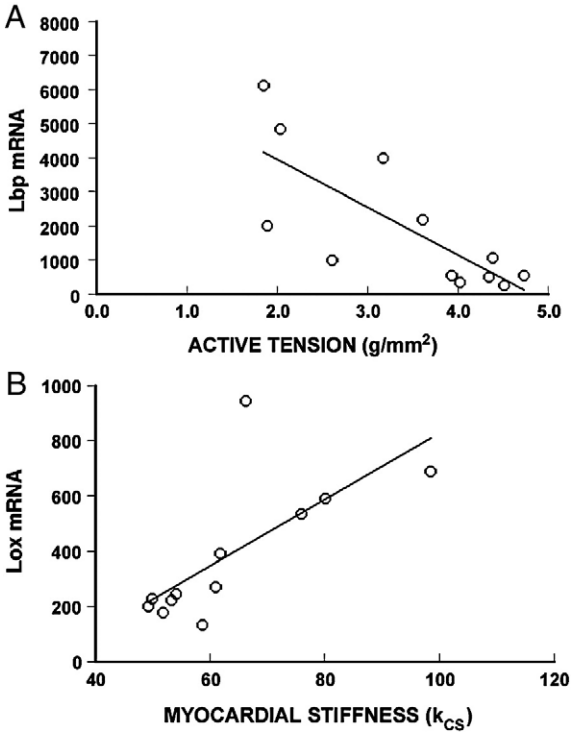

Fig. 5. (A) Example of regression plot between expression intensity of lipopolysaccharide binding protein (Lbp level determined by gene chip) and active tension of LV papillary muscle is shown in the top panel. (B) Expression of lysyl oxidase (Lox level determined by gene chip) and myocardial stiffness of LV papillary muscle is shown in the bottom panel. These values represent individual LV gene expression and papillary muscle function data obtained from the same heart.

LV remodeling

Histological data from LV and papillary muscles [4] indicate that fibrosis and hypertrophy are well established in the compensated SHR and increases further with HF. It is of interest that progressive myocardial fibrosis and the transition to HF can be prevented in aging SHR hearts if treatment with the ACE inhibitor captopril is begun at 12 to14 months of age, or prior to the development of failure [4], consistent with the recognized importantance of the renin–angiotensin–aldosterone system in hypertension induced LV remodeling [24,29]. In the present study, the increase in ECM-related transcripts (e.g. lysyl oxidase (Lox), thrombospondin (Thbs4), cathepsins (Ctss)) in SHR-F vs. SHR-NF correspond to a progression of fibrosis and indicates that the ECM response is continuing to evolve with the development of systolic HF. Thrombospondin-4 (Thbs4), which was found to increase 1.8-fold in 20-month-old SHR vs.16-month-old animals [20] was increased more than 3 fold in SHR-F vs. SHR-NF. Fibronectin-1, which was up-regulated by 1.5 fold between 20- and 16-month-old SHR [20] was 3.65-fold greater in SHR-F vs. non failing SHR. The composition of the ECM as well as the extent of fibrosis may alter cardiac function and myocardial stiffness. The expression of the collagen cross-linking enzyme lysyl oxidase (Lox) was positively correlated with myocardial stiffness noted in the present papillary muscle studies (Fig. 5B). Lysyl oxidase inhibition with BAPN, a collagen crosss-link inhibitor, has been shown to modify myocardial stiffness of hypertrophied hearts [42]. Lysyl oxidase is up-regulated in human HF [28] and was highly expressed in the SHR-F group. Up-regulated ECM transcripts have previously been reported in the SHR with diastolic dysfunction [20]; there are differences comparing age-matched non-failing and failing SHR in the present study, possibly consistent with the concept of a progression from diastolic dysfunction reported by Rysa [20] to systolic dysfunction in the present study.

Conclusions

This investigation describes for the first time the association between functional and structural changes and alternations in gene expression associated with the development of systolic dysfunction in the aging SHR model of hypertensive HF. Furthermore, the study demontrates the relationship between systolic dysfunction in the intact animal and impairment of intrinsic myocardial contractile properties. The spectrum of changes in gene expression reported in the SHR with diastolic dysfunction is expanded to include a broad spectrum of transcript changes involving many processes including inflammation, apoptosis, oxidative stress and altered cell signaling pathways in addition to a further upregulation of ECM transcripts, occurring with the development of systolic dysfunction. While some transcriptional changes associated with systolic HF may be secondary, GSEA findings support the concept that these identified pathways and mechanisms may play an important role in myocardial dysfunction and adverse remodeling associated with hypertensive HF.

Materials and methods

Animal model

Sixteen male SHR were purchased from Taconic (Germantown, NY). All rats were housed two per container and fed regular rat chow and water with a 12-h light/dark cycle. All animal experiments were performed in accordance with the NIH Guide for the Care and Use of Laboratory Animals and were approved by the Animal Studies Committee at the Boston VA Healthcare System. Animals were monitored several times per week for the presence of tachypnea and labored respiration, body weight and blood pressure (indirect tail cuff method) were determined monthly. Animals underwent echocardiographic study every 4 to 6 weeks or upon demonstration of respiratory changes. Those animals found to have HF were studied at

the time of HF, and compared to age-matched SHR without HF. Four SHR died prior to study.

Echocardiography

Chamber dimensions and LV function were measured using transthoracic echocardiography as previously described [3,4]. Briefly, rats were lightly anesthetized with isoflurane (1.5% to 2% by O_2 inhalation) and placed in the supine position. 2D guided M-mode studies were performed using a 10-MHz linear array transducer and images at the tip of the left ventricular papillary muscle recorded. The thickness of the posterior and anterior walls of the LV chamber and the LV chamber diameter during systole and diastole were measured. All parameters were measured over at least six consecutive cardiac cycles. Averages were used to calculate LV ejection fraction, LV fractional shortening, LV end-diastolic and systolic diameters, and LV systolic and diastolic volumes.

Isolated muscle studies

After echocardiography, the hearts were quickly removed, weighed, and placed in oxygenated Krebs–Henseleit solution at 28 °C. The LV posterior papillary muscle was dissected free, mounted between two spring clips, and placed vertically in a 100-ml acrylic chamber containing oxygenated Krebs–Henseleit solution, and then attached to a low-inertia DC pen motor and semiconductor strain gauge force transducer as previously described [4,23]. A digital computer with an analog/digital interface allowed control of either force or length of the preparation. Force and length data were sampled at a rate of 1.0 kHz and stored on disk for later analysis. A central segment scanning system was utilized to measure passive stiffness of the central segment of the papillary muscle (k_{cs}) as previously described [22,23].

Force–velocity relations (shortening velocity vs. load) were determined from muscle shortening velocity measurements following "quick releases" 100 ms after stimulation to loads ranging from 0.5 g to peak isometric force. Values were subsequently normalized for muscle length and cross-sectional area, as described previously [22,23].

cDNA microarray

Samples of LV tissue were obtained at the time of study and immediately frozen in liquid nitrogen. Total RNA was isolated from approximately 30 mg of frozen left ventricle using RNeasy mini columns for fibrous tissue (Qiagen, Valencia, CA). 30 mg of frozen tissue was pulverized and transferred to a tube containing 300 :l RLT buffer. The sample was homogenized using a Omni PCR homogenizer (Omni International). Debris was removed from the lysate using QIA shredder (Qiagen) following proteinase K digestion at 55 °C for 10 min. Total RNA was isolated using the RNeasy spin columns following on-column DNase treatment to remove any contaminating DNA. The integrity and concentration of the different RNA samples were determined using RNA Nano LabChip (Agilent Technologies, Inc., Santa Clara, CA). Individual samples containing equal amounts of total RNA from each LV were prepared. Expression values were compared between two groups of animals: non-failing SHR and un-treated SHR with heart failure. Target preparation, hybridization to the Affymetrix 230 2.0 array, and detection was performed by the Genomics Department at Boston University School of Medicine. All hybridizations were performed on six individual samples for each of two groups (total of 12 independent hybridizations). The normalized array data and raw data files are available from GEO. The GEO serial number is GSE19210.

Microarray quantification, normalization and analysis

Transcript-level expression estimates of the probe-level hybridization intensities were derived using the MAS 5 algorithm in Affymetrix GeneChip software (version 3.3; Affymetrix, Santa Clara, CA). Only those transcripts that were detected above background in at least one sample (i.e. at least one sample had an MAS 5 detection call of "present") were included in subsequent analyses. Statistically significant differences in mean values were tested by Student's t-test and corrected for multiple comparisons using the False Discovery Rate (FDR) method of Benjamini and Hochberg [43]. An FDR<0.05 was considered evidence of statistically significant differential expression between groups. For each gene, the p value was used to determine significance rather than fold change, in order to maximize the proportion of candidate gene changes.

To identify the enriched gene sets, pathways or GO term gene functions, the gene set enrichment analysis method [21] was adopted. This bioinformatic tool evaluates all significantly measured targets derived from a microarray experiment at the level of gene sets, which are defined based on prior biological knowledge. GSEA determines whether genes belonging to a biological pathway or a previously determined functional group are significantly over-represented at the top or bottom of a ranked gene list compared to controls without a predefined cut-off value. Thus, biologically relevant information is not missed by losing target genes due to an "arbitrarily" chosen cut-off value. The two curated gene sets C2 and C5 (i.e. SHR with HF vs. SHR without HF) within the up-to-date molecular signature database (MSigDB-v2.5: http://www.broadinstitute.org/gsea/msigdb/index.jsp) was used to perform such enrichment analysis for either pathways or GO term functions, respectively. All parameters in the analysis were set to default.

Quantitative real-time PCR

To independently confirm the differential expression data obtained by microarray analysis, real time quantitative reverse transcription (RT)-PCR was utilized to determine the relative expression of selected genes. cDNA for RT-PCR was produced using 1 μg of total RNA in a 20: l reaction containing first strand buffer, dTTP, dATP, dGTP and dCTP (final concentration, 0.4 mM each), 100 U of Superscript II (Life technologies), 10 U of RNase inhibitor, 500 ng of random hexamer. The cDNA synthesis reaction mixture was incubated at 42 °C for 1 h. Then, real-time PCR was carried out in the presence of specific primers for each transcript. RT-PCR was performed in triplicate on 10 ng of each cDNA with the SYBR Green master mix using the LightCycler PCR system following the manufacturer's instructions (Roche Diagnostics, Mannheim, Germany). To insure that there was no genomic contamination of cDNA and no primer dimer artifact, real-time reactions containing cDNA generated without reverse transcriptase and reactions containing primers alone were also included. All PCR reactions were repeated six times per sample, and expression level normalized to 18 S expression with the standard curve method. The resulting averages between groups were then compared statistically.

Pathological and histological analysis of hearts and liver

After removal of the papillary muscles, the right ventricle (RV) and left ventricle (LV) were carefully separated. Myocardial and liver tissue samples were gently blotted and weighed. LV and RV wet weight normalized by body weight (e.g. LV/BW and RV/BW) and LV by tibia length (LV/TL) were used as indices of ventricular hypertrophy. Water content of tissue samples was determined as previously described [22].

Samples of LV free wall were placed in 10% formalin fixative, and prepared for microscopy and histological analysis as previously described [4,23,24]. At the conclusion of the mechanical studies, the central segment of the LV papillary muscle was fixed with a preload equivalent to the resting stress at L_{max}. Histological sections of the central segment of LV papillary muscles were stained with Masson's trichrome. Areas of connective tissue network and myocytes were quantified by a semiautomated computer-based video analysis system with an Image-Pro Plus software package (Silver Spring, MD).

Statistical analysis

Data are expressed as mean ± SD unless otherwise stated. Data set comparisons were performed with Student's unpaired, two-tailed *t*-test. Differences in mean values were considered statistically significant at a probability level of less than 5% ($p<0.05$).

Acknowledgments

This work was supported by Medical Research Funds provided to WWB from the Department of Veterans Affairs. We are particularly grateful to Dr. Marc Lenburg of the Genomics Department at Boston University School of Medicine for his help in carrying out the data acquisition and statistical analysis of the Affymetrix GeneChip data.

Appendix A. Supplementary data

Supplementary data associated with this article can be found, in the online version, at doi:10.1016/j.ygeno.2009.12.002.

References

[1] N.C. Trippodo, E.D. Frohlich, Similarities of genetic (spontaneous) hypertension. Man and rat, Circ. Res. 48 (1981) 309–319.
[2] J.M. Pfeffer, M.A. Pfeffer, I. Mirsky, E. Braunwald, Regression of left ventricular hypertrophy and prevention of left ventricular dysfunction by captopril in the spontaneously hypertensive rat, Proc. Natl. Acad. Sci. U. S. A. 79 (1982) 3310–3314.
[3] O.H. Bing, W.W. Brooks, K.G. Robinson, M.T. Slawsky, J.A. Hayes, S.E. Litwin, S. Sen, C.H. Conrad, The spontaneously hypertensive rat as a model of the transition from compensated left ventricular hypertrophy to failure, J. Mol. Cell. Cardiol. 27 (1995) 383–396.
[4] W.W. Brooks, O.H. Bing, K.G. Robinson, M.T. Slawsky, D.M. Chaletsky, C.H. Conrad, Effect of angiotensin-converting enzyme inhibition on myocardial fibrosis and function in hypertrophied and failing myocardium from the spontaneously hypertensive rat, Circulation 96 (1997) 4002–4010.
[5] J.J. Hwang, P.D. Allen, G.C. Tseng, C.W. Lam, L. Fananapazir, V.J. Dzau, C.C. Liew, Microarray gene expression profiles in dilated and hypertrophic cardiomyopathic end-stage heart failure, Physiol. Genomics 10 (2002) 31–44.
[6] M. Steenman, Y.W. Chen, M. Le Cunff, G. Lamirault, A. Varro, E. Hoffman, J.J. Leger, Transcriptomal analysis of failing and nonfailing human hearts, Physiol. Genomics 12 (2003) 97–112.
[7] M. Wellner, R. Dechend, J.K. Park, E. Shagdarsuren, N. Al-Saadi, T. Kirsch, P. Gratze, W. Schneider, S. Meiners, A. Fiebeler, H. Haller, F.C. Luft, D.N. Muller, Cardiac gene expression profile in rats with terminal heart failure and cachexia, Physiol. Genomics 20 (2005) 256–267.
[8] S. Ueno, R. Ohki, T. Hashimoto, T. Takizawa, K. Takeuchi, Y. Yamashita, J. Ota, Y.L. Choi, T. Wada, K. Koinuma, K. Yamamoto, U. Ikeda, K. Shimada, H. Mano, DNA microarray analysis of in vivo progression mechanism of heart failure, Biochem. Biophys. Res. Commun. 307 (2003) 771–777.
[9] S.W. Kong, N. Bodyak, P. Yue, Z. Liu, J. Brown, S. Izumo, P.M. Kang, Genetic expression profiles during physiological and pathological cardiac hypertrophy and heart failure in rats, Physiol. Genomics 21 (2005) 34–42.
[10] Z. Tang, B.S. McGowan, S.A. Huber, C.F. McTiernan, S. Addya, S. Surrey, T. Kubota, P. Fortina, Y. Higuchi, M.A. Diamond, D.S. Wyre, A.M. Feldman, Gene expression profiling during the transition to failure in TNF-alpha over-expressing mice demonstrates the development of autoimmune myocarditis, J. Mol. Cell. Cardiol. 36 (2004) 515–530.
[11] S. Schiekofer, I. Shiojima, K. Sato, G. Galasso, Y. Oshima, K. Walsh, Microarray analysis of Akt1 activation in transgenic mouse hearts reveals transcript expression profiles associated with compensatory hypertrophy and failure, Physiol. Genomics 27 (2006) 156–170.
[12] Z. Gao, H. Xu, D. DiSilvestre, V.L. Halperin, R. Tunin, Y. Tian, W. Yu, R.L. Winslow, G.F. Tomaselli, Transcriptomic profiling of the canine tachycardia-induced heart failure model: global comparison to human and murine heart failure, J. Mol. Cell. Cardiol. 40 (2006) 76–86.
[13] C. Ojaimi, K. Qanud, T.H. Hintze, F.A. Recchia, Altered expression of a limited number of genes contributes to cardiac decompensation during chronic ventricular tachypacing in dogs, Physiol. Genomics 29 (2007) 76–83.
[14] S. Zicha, L. Xiao, S. Stafford, T.J. Cha, W. Han, A. Varro, S. Nattel, Transmural expression of transient outward potassium current subunits in normal and failing canine and human hearts, J. Physiol. 561 (2004) 735–748.
[15] F.G. Akar, R.C. Wu, G.J. Juang, Y. Tian, M. Burysek, D. Disilvestre, W. Xiong, A.A. Armoundas, G.F. Tomaselli, Molecular mechanisms underlying K+ current downregulation in canine tachycardia-induced heart failure, Am. J. Physiol. Heart. Circ. Physiol. 288 (2005) H2887–96.
[16] A. Garnier, D. Fortin, C. Delomenie, I. Momken, V. Veksler, R. Ventura-Clapier, Depressed mitochondrial transcription factors and oxidative capacity in rat failing cardiac and skeletal muscles, J. Physiol. 551 (2003) 491–501.
[17] B. Lei, V. Lionetti, M.E. Young, M.P. Chandler, C. d'Agostino, E. Kang, M. Altarejos, K. Matsuo, T.H. Hintze, W.C. Stanley, F.A. Recchia, Paradoxical downregulation of the glucose oxidation pathway despite enhanced flux in severe heart failure, J. Mol. Cell. Cardiol. 36 (2004) 567–576.
[18] C.C. Strom, M. Aplin, T. Ploug, T.E. Christoffersen, J. Langfort, M. Viese, H. Galbo, S. Haunso, S.P. Sheikh, Expression profiling reveals differences in metabolic gene expression between exercise-induced cardiac effects and maladaptive cardiac hypertrophy, FEBS J. 272 (2005) 2684–2695.
[19] J.L. Samuel, M.C. Schaub, M. Zaugg, M. Mamas, W.B. Dunn, B. Swynghedauw, Genomics in cardiac metabolism, Cardiovasc. Res. 79 (2008) 218–227.
[20] J. Rysa, H. Leskinen, M. Ilves, H. Ruskoaho, Distinct upregulation of extracellular matrix genes in transition from hypertrophy to hypertensive heart failure, Hypertension 45 (2005) 927–933.
[21] A. Subramanian, P. Tamayo, V.K. Mootha, S. Mukherjee, B.L. Ebert, M.A. Gillette, A. Paulovich, S.L. Pomeroy, T.R. Golub, E.S. Lander, J.P. Mesirov, Gene set enrichment analysis: a knowledge-based approach for interpreting genome-wide expression profiles, Proc. Natl. Acad. Sci. U. S. A. 102 (2005) 15545–15550.
[22] C.H. Conrad, W.W. Brooks, K.G. Robinson, O.H. Bing, Impaired myocardial function in spontaneously hypertensive rats with heart failure, Am. J. Physiol. 260 (1991) H136–45.
[23] C.H. Conrad, W.W. Brooks, J.A. Hayes, S. Sen, K.G. Robinson, O.H. Bing, Myocardial fibrosis and stiffness with hypertrophy and heart failure in the spontaneously hypertensive rat, Circulation 91 (1995) 161–170.
[24] W.W. Brooks, O.H. Bing, C.H. Conrad, L. O'Neill, M.T. Crow, E.G. Lakatta, D.E. Dostal, K.M. Baker, M.O. Boluyt, Captopril modifies gene expression in hypertrophied and failing hearts of aged spontaneously hypertensive rats, Hypertension 30 (1997) 1362–1368.
[25] U.C. Sharma, S. Pokharel, C.T. Evelo, J.G. Maessen, A systematic review of large scale and heterogeneous gene array data in heart failure, J. Mol. Cell. Cardiol. 38 (2005) 425–432.
[26] H. Jin, R. Yang, T.A. Awad, F. Wang, W. Li, S.P. Williams, A. Ogasawara, B. Shimada, P.M. Williams, G. de Feo, N.F. Paoni, Effects of early angiotensin-converting enzyme inhibition on cardiac gene expression after acute myocardial infarction, Circulation 103 (2001) 736–742.
[27] M. Rauchhaus, W. Doehner, D.P. Francis, C. Davos, M. Kemp, C. Liebenthal, J. Niebauer, J. Hooper, H.D. Volk, A.J. Coats, S.D. Anker, Plasma cytokine parameters and mortality in patients with chronic heart failure, Circulation 102 (2000) 3060–3067.
[28] P. Sivakumar, S. Gupta, S. Sarkar, S. Sen, Upregulation of lysyl oxidase and MMPs during cardiac remodeling in human dilated cardiomyopathy, Mol. Cell. Biochem. 307 (2008) 159–167.
[29] M.O. Boluyt, L. O'Neill, A.L. Meredith, O.H. Bing, W.W. Brooks, C.H. Conrad, M.T. Crow, E.G. Lakatta, Alterations in cardiac gene expression during the transition from stable hypertrophy to heart failure. Marked upregulation of genes encoding extracellular matrix components, Circ. Res. 75 (1994) 23–32.
[30] M.R. Bergman, R.H. Kao, S.A. McCune, B.J. Holycross, Myocardial tumor necrosis factor-alpha secretion in hypertensive and heart failure-prone rats, Am. J. Physiol. 277 (1999) H543–50.
[31] K.R. Feingold, Y. Wang, A. Moser, J.K. Shigenaga, C. Grunfeld, LPS decreases fatty acid oxidation and nuclear hormone receptors in the kidney, J. Lipid. Res. 49 (2008) 2179–2187.
[32] K. Sekiguchi, Q. Tian, M. Ishiyama, J. Burchfield, F. Gao, D.L. Mann, P.M. Barger, Inhibition of PPAR-alpha activity in mice with cardiac-restricted expression of tumor necrosis factor: potential role of TGF-beta/Smad3, Am. J. Physiol. Heart. Circ. Physiol. 292 (2007) H1443–51.
[33] M.P. Gupta, S.A. Samant, S.H. Smith, S.G. Shroff, HDAC4 and PCAF bind to cardiac sarcomeres and play a role in regulating myofilament contractile activity, J. Biol. Chem. 283 (2008) 10135–10146.
[34] X.W. Cheng, K. Obata, M. Kuzuya, H. Izawa, K. Nakamura, E. Asai, T. Nagasaka, M. Saka, T. Kimata, A. Noda, K. Nagata, H. Jin, G.P. Shi, A. Iguchi, T. Murohara, M. Yokota, Elastolytic cathepsin induction/activation system exists in myocardium and is upregulated in hypertensive heart failure, Hypertension 48 (2006) 979–987.
[35] M. Kamisago, J.P. Schmitt, D. McNamara, C. Seidman, J.G. Seidman, Sarcomere protein gene mutations and inherited heart disease: a beta-cardiac myosin heavy chain mutation causing endocardial fibroelastosis and heart failure, Novartis. Found. Symp. 274 (2006) 176–189 discussion 189-95, 272-6.
[36] N. Maitra, C. Adamson, K. Greer, S. Klewer, J. Hoying, J.J. Bahl, S. Goldman, E. Morkin, Regulation of gene expression in rats with heart failure treated with the thyroid hormone analog 3,5-diiodothyropropionic acid (DITPA) and the combination of DITPA and captopril, J. Cardiovasc. Pharmacol. 50 (2007) 526–534.
[37] H. Tsutsui, S. Kinugawa, S. Matsushima, Mitochondrial oxidative stress and dysfunction in myocardial remodelling, Cardiovasc. Res. 81 (2009) 449–456.
[38] M.E. Young, P. McNulty, H. Taegtmeyer, Adaptation and maladaptation of the heart in diabetes: Part II: potential mechanisms, Circulation 105 (2002) 1861–1870.
[39] G. Ding, M. Fu, Q. Qin, W. Lewis, H.W. Kim, T. Fukai, M. Bacanamwo, Y.E. Chen, M.D. Schneider, D.J. Mangelsdorf, R.M. Evans, Q. Yang, Cardiac peroxisome proliferator-activated receptor gamma is essential in protecting cardiomyocytes from oxidative damage, Cardiovasc. Res. 76 (2007) 269–279.
[40] J. Marin-Garcia, M.J. Goldenthal, Mitochondrial centrality in heart failure, Heart Fail. Rev. 13 (2008) 137–150.
[41] Y. Chen, S. Park, Y. Li, E. Missov, M. Hou, X. Han, J.L. Hall, L.W. Miller, R.J. Bache, Alterations of gene expression in failing myocardium following left ventricular assist device support, Physiol. Genomics 14 (2003) 251–260.
[42] O.H. Bing, B.L. Fanburg, W.W. Brooks, S. Matsushita, The effect of lathyrogen beta-amino proprionitrile (BAPN) on the mechanical properties of experimentally hypertrophied rat cardiac muscle, Circ. Res. 43 (1978) 632–637.
[43] H.Y. Benjamini, Controlling the false discovery rate: a practical and powerful approach to multiple testing, J. Royal. Statistical. Soc. B 57 (1995) 289–300.